

## Journal Pre-proofs

Experimental study of the bond interaction between CFRP and concrete under blast loading

Azer Maazoun, Stijn Matthys, Bachir Belkassem, Oussama Atoui, David Lecompte

PII: S0263-8223(21)01070-9  
DOI: <https://doi.org/10.1016/j.compstruct.2021.114608>  
Reference: COST 114608

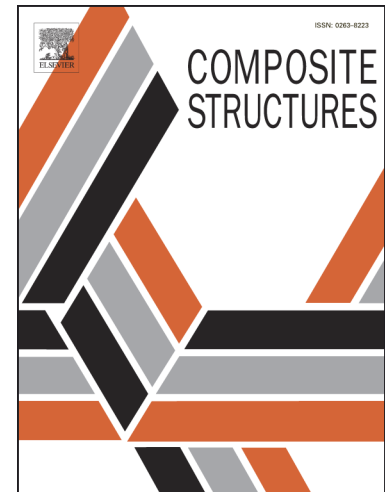
To appear in: *Composite Structures*

Received Date: 23 September 2020  
Revised Date: 14 August 2021  
Accepted Date: 22 August 2021

Please cite this article as: Maazoun, A., Matthys, S., Belkassem, B., Atoui, O., Lecompte, D., Experimental study of the bond interaction between CFRP and concrete under blast loading, *Composite Structures* (2021), doi: <https://doi.org/10.1016/j.compstruct.2021.114608>

This is a PDF file of an article that has undergone enhancements after acceptance, such as the addition of a cover page and metadata, and formatting for readability, but it is not yet the definitive version of record. This version will undergo additional copyediting, typesetting and review before it is published in its final form, but we are providing this version to give early visibility of the article. Please note that, during the production process, errors may be discovered which could affect the content, and all legal disclaimers that apply to the journal pertain.

© 2021 Elsevier Ltd. All rights reserved.



# Experimental study of the bond interaction between CFRP and concrete under blast loading

**Azer Maazoun** <sup>12\*</sup>, Ph-D

<sup>1</sup>Ghent University, Magnel-Vandepitte Laboratory, Department of Structural Engineering and Building materials, Technologie park-Zwijnaarde 904, 9052 Gent, Belgium, [azer.maazoun@ugent.be](mailto:azer.maazoun@ugent.be)

<sup>2</sup>Science and Technology for Defense Laboratory, Center for Military Research, Tunisia

**Stijn Matthys**, Professor

Ghent University, Magnel-Vandepitte Laboratory, Department of Structural Engineering and Building materials, Technologie park-Zwijnaarde 904, 9052 Gent, Belgium, [stijn.matthys@ugent.be](mailto:stijn.matthys@ugent.be)

**Bachir Belkassem**, Researcher

Royal Military Academy, Civil and Materials Engineering Department, 30 Avenue de la renaissance, 1000 Brussels, Belgium, [bachir.belkassem@rma.ac.be](mailto:bachir.belkassem@rma.ac.be)

**Oussama Atoui**, PhD student

Royal Military Academy, Civil and Materials Engineering Department, 30 Avenue de la renaissance, Belgium, [oussama.atoui@rma.ac.be](mailto:oussama.atoui@rma.ac.be)

**David Lecompte**, Professor

Royal Military Academy, Civil and Materials Engineering Department, 30 Avenue de la renaissance, 1000 Brussels, Belgium, [david.lecompte@mil.be](mailto:david.lecompte@mil.be)

---

\* Corresponding author,

Military Academy of Fondouk Jedid, Civil Engineering Department, 8021 Nabeul, Tunisia

Tel : +216 29 700 034, E-mail : [azer.maazoun@ugent.be](mailto:azer.maazoun@ugent.be)

## Abstract

Specific to blast loading, bond shear tests between carbon fiber reinforced polymer (CFRP) strips and concrete have not yet been reported in literature, to the best knowledge of the authors. Given the high potential of strengthening concrete with CFRP to increase blast resistance, it is necessary to better understand the dynamic interaction between concrete and CFRP under blast impulse. This article presents a new experimental setup developed in order to study blast driven bond interaction between CFRP and concrete. An evaluation of the bond at the interface between the CFRP strip and the concrete is conducted in order to identify the parameters that affect the bond strength under blast loading. Several retrofitted specimens with different bond strength are tested. An explosive driven shock tube (EDST) set-up is used to generate the blast loading. Piezo resistive strain gauges and digital image correlation (DIC) measurement are used to record the debonding process and the evolution of the strain along the bonded area. As such, the bond behaviour is studied for three different bond lengths and the effect of interaction of the blast wave within the concrete is highlighted. The experimental tests demonstrate that under blast loading, the debonding between the CFRP strip and the concrete occurs due to a combined effect: interface stresses caused by the induced force in the CFRP and additional stresses resulting from the propagation of the blast induced stress wave within the concrete.

## 1. Introduction

Fiber reinforced polymer (FRP) as externally bonded reinforcement (EBR) has become a mainstream technology over the last decades to retrofit concrete structures and is also applicable to the case of blast loading [1–4]. Its effectiveness for strengthening against blast loads is of importance to the building sector, as well as to society from a security and safety perspective. The advantages of FRP as EBR are the high strength, the low weight and the excellent durability characteristics in combination with their ease of application. Furthermore, they allow to increase the resilience of existing structures against blast loading by adding strength, stiffness and energy dissipation.

Several studies are reported about the use of carbon fiber reinforced polymer (CFRP) as EBR for strengthening reinforced concrete structures against blast loading, and application examples are mentioned in [4–8] and the lack of understanding on CFRP debonding under blast impulse follows e.g

from [9-12]. J.Ha et al. [9] tested nine RC specimens with dimensions of 1 m x 1 m x 0.15 m retrofitted with either CFRP, polyurea (PU) or hybrid CFRP/PU under blast loading. The blast load was generated by detonating a 15.88 kg of ammonium nitrate of fuel oil (ANFO) at 1.5 m standoff distance on the opposite side where the CFRP and PU are bonded. From the test results, the maximum displacement of CFRP, PU and hybrid CFRP/PU specimens with respect to the reference specimen decreased by 21.4%, 15.7%, and 37.4%, respectively. Moreover, the energy absorption capacity of a retrofitted specimen, defined as the ratio of the difference between maximum and residual displacement to maximum displacement were 79.9%, 67.14%, and 71.8% for CFRP, PU, and hybrid CFRP/PU specimens, respectively. They observed that using the hybrid CFRP/PU offered an excellent blast protection, compared to the other strengthening techniques. However, local debonding was reported after each explosion at the edge of the retrofitted specimens without giving a further explanation on the reason of this failure aspect. It is not well understood why blast loading often leads to the ripping off of the EBR. Nam et al. [10] developed a numerical model for RC slabs retrofitted with GFRP and compared the numerical model with a previous experimental result conducted by Razaqpur et al. [11]. The FRP retrofitting effectiveness is evaluated by using different FRP failure models. They found that more research is required to improve their FE model on the dynamic interfacial behaviour between FRP and concrete due the complexity of the problem and they suggested that a dynamic pull-out test could be experimentally developed in order to obtain the dynamic interfacial behaviour between concrete and FRP. De Lorenzis [12] developed an analytical bond slip model for shear bond slip test (pull out test) under impulsive loads, based on the bond slip relationship developed for the static loads. However, this model is restricted by several assumptions (the softening region of the bond slip model is not considered; the bond length of the CFRP strip is significantly longer than the effective bond length; the effect of the longitudinal waves is neglected; the elastic waves generated by the impulse load propagate with a constant speed along the adhesive bond between CFRP and concrete) which affect the accuracy of the analytical results and which were not verified experimentally.

These previous studies show that some progress has been made to study the behaviour of the adhesive bond between concrete and CFRP strips under blast loading. However, it appears that there is a lack of

understanding on the bond behaviour of FRP strengthened structures under blast loading. This can be related to the high costs of the experiments, the sometimes confidential nature of this type of research and the many difficulties in getting reliable experimental results due to the destructive nature and the short duration of the explosion load [13].

Bond strength evaluation techniques under dynamic regime have been explored by the use of pulsed laser [14], plate impact [15] or high power electrical generators [16] but never with blast loading. In these previous studies, the mechanical wavelength was lower than the thickness of the material layers and thus, the main mechanism involved in the bond damage is spallation. These methods remain out of range for testing sample of the characteristic size of civil engineering structures. Using a longer mechanical impulse, like the one caused by the blast structure interaction, would allow extending dynamic adhesion tests to larger structures. The problem of the bond strength has been poorly investigated under blast loading specifically. Such bond shear blast tests are required to understand the dynamic interaction between concrete and CFRP further. In this article, the evolution of the bond at the interface between the CFRP strips and the concrete under blast loading is conducted. A double bond shear test is developed using an explosive driven shock tube (EDST) set-up to test the bond interface under blast loading. Piezo resistive strain gauges and DIC measurement are used to record the debonding process and the evolution of the strain along the bonded area. As such, the bond behaviour is studied for three different bond lengths and the effect of interaction of the blast wave within the concrete is highlighted. Details of the test set-up are reported, as well as the experimental results conducted on nine specimens.

## **2. Experimental analysis of the bond slip between CFRP and concrete under blast loading**

### **2.1 Specimen design**

In order to investigate the behaviour of the bond between the CFRP strip and the concrete under blast loading, a dedicated test methodology has been developed. Details of the novel set-up are provided in the section 2.2. Nine concrete prisms are casted in laboratory conditions with the following dimensions: length 220 mm, width 150 mm and height 150 mm. A compressive concrete strength of 53.3 MPa is

obtained at age of the bond tests (65 days, average of 3 cubes with side length 150 mm). Figure 1 shows the concrete prism dimensions, as well as the surface aspect of the roughened concrete.

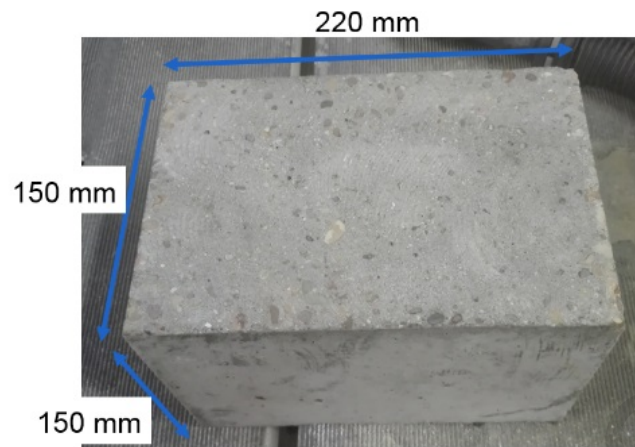


Figure 1. Concrete prisms dimensions

Before bonding the CFRP strips, the concrete surface has been roughened using a diamond disc grinder in order to expose the aggregates and promote mechanical anchoring between CFRP and concrete in an optimum way. Next, a vacuum cleaning is applied to make the concrete dust free. Before the adhesion of the FRP strips, the strips are cleaned with acetone to remove any traces of grease and dust. The epoxy Sikadur® 30 is mixed in the specified proportions (25% mass of hardener and 75% mass of the resin are mixed for 3 minutes until obtaining a uniform colour of the mixture). After limiting the bonded area with tape, a thin layer of adhesive is applied on the roughened and cleaned concrete surface and a layer of adhesive is applied on the FRP strip in a dome shape, reducing the risk of forming voids. After that, the strip is placed on the concrete surface and a rubber roller is used to apply a pressure on the strip to ensure an intimate contact. The extra epoxy that slurred out of the CFRP is removed. No pressing devices were applied during the curing process. After reticulation (10 days), the tape is removed and an average bond thickness of 1.5 mm is measured in all retrofitted concrete prism. Note that the bonding process is carried out at the ambient temperature of the laboratory 25 °C. Three series of tests are performed (A, B and C) with a given width of 50 mm and different bond lengths (50 mm, 100 mm and 200 mm) and each test is repeated three times. Figure 2 shows the specimens before the blast tests. Note that the CFRP strip is bonded over the full contact surface with the concrete, and has no small unbonded zone at the loaded end as often is considered in static bond shear tests. For the case of the blast loading, the small unbonded

zone is avoided because it could create a small gap in which the blast wave could additionally penetrate and cause local stress deviations. This could trigger a crack initiation and could modify the bond strength of the retrofitted concrete prism.

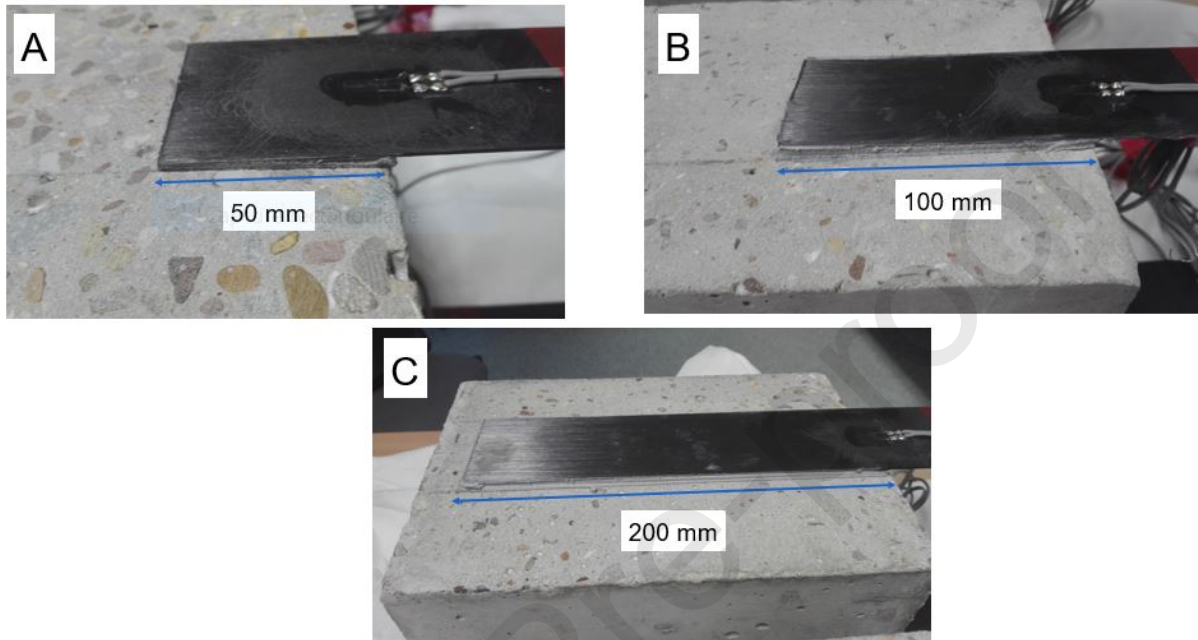


Figure 2. Retrofitted concrete prisms with different bond lengths

For CFRP strips, prefabricated unidirectional Sika CarboDur S512 plates have been used with the following dimensions 50 mm width, 1.2 mm thickness and 900 mm length. According to the technical data provided by the supplier, the CFRP strips have a density of 1650 kg/m<sup>3</sup> and a carbon fibre volumetric content equal to 70%. For the concrete prism, the concrete was prepared with cement, gravel with a maximum aggregate size of 16 mm, sand, water and superplasticisers. The mix proportion of the constituents and quantities for each concrete prism are summarised in Table 1.

Table 1. Mix proportions of the concrete

Component	sand	cement	Coarse aggregate	Fine aggregate	water	superplasticisers
Mass [kg]	4.5	2.25	2.1	4.5	0.9	0.0045

The quasi-static mechanical material properties of the CFRP, the epoxy and the concrete are shown in Table 2. The properties of the CFRP strips and adhesive are obtained from the manufactures, while those of the concrete followed from lab testing according to the standard NF EN 12 390 – 3.

Table 2. quasi-static mechanical material properties

Materials	Young modulus (MPa)	Compressive strength (MPa)	Tensile strength (MPa)	Thickness (mm)	Width (mm)
Concrete	36300	53.3	3.8	-	-
CFRP	165000	-	2800	1.2	50
Epoxy (Sikadur30)	11200	30	70	1.5	

## 2.2 Description of the experimental setup for the blast tests

In this study, double bond shear tests are performed [17]. An explosive driven shock tube (EDST) is used to generate a uniform blast wave [18] while reducing the light and the smoke of the explosion that screens the camera field. Two Photron SA5 high-speed cameras are used for recording the evolution of the strain in the CFRP strip using DIC measurement. Figures 3 and 4 show the experimental setup. A fixed steel frame is used to clamp the CFRP strips. The CFRP strips are clamped using steel plates with the following dimensions: length 140 mm, width 100 mm and thickness 5 mm. A torque wrench is used to apply a specific torque of 50 N.m to fasten the bolts and tighten the CFRP strips to the fixed steel frame. Moreover, an aluminium alloy plate “EN AW 7075” with a U shape is placed between the end of the tube and the concrete prism, to avoid the impact of the blast wave on the lateral side of the CFRP strips. The aluminium alloy plate has the following dimensions: length 150 mm, width 100 mm and thickness 18 mm. To allow the displacement of the concrete prism, the latter is roller supported so that it can freely move in translation by the blast wave generated by the EDST. The EDST has a square section with the following dimensions; the width is 80 mm, the thickness of the tube wall is 5 mm, and the length is 1 m.

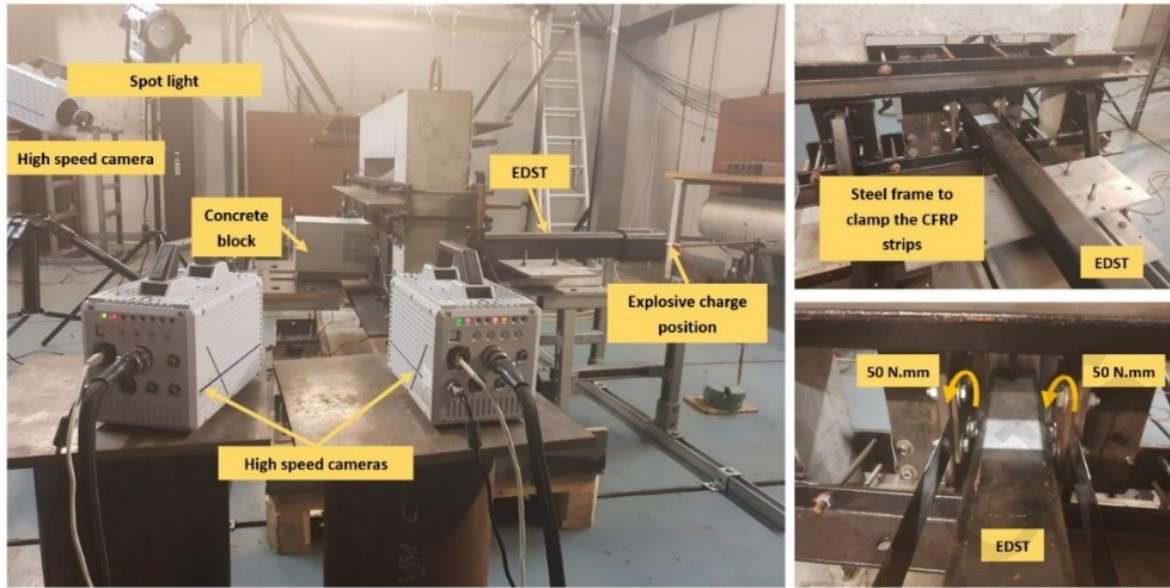


Figure 3. Experimental setup for the bond slip tests under blast loads

In order to avoid torsion at the interface and having a pure shear failure mechanism between the CFRP strips and the concrete prism, a laser beam is used to enhance the alignment between the EDST, the aluminium plate and the concrete prism. A schematic representation of the setup is shown in Figure 4.

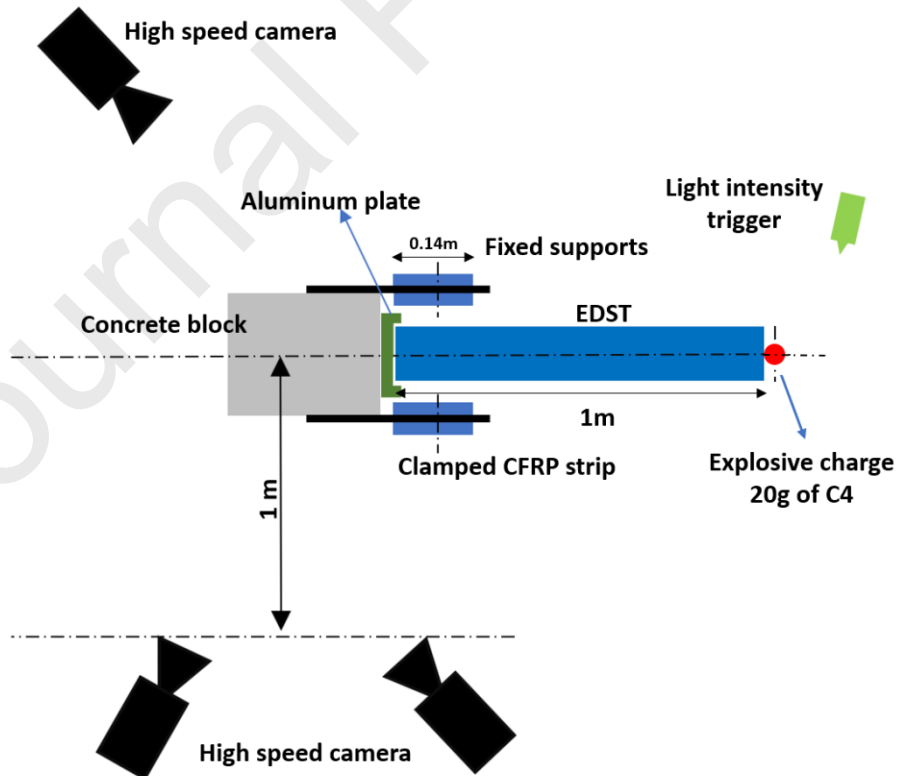


Figure 4. A schematic representation of the blast setup

### 2.3 Instrumentation

Figure 5 shows the deformation measurements equipment used in the blast tests. DIC is used to obtain the displacements (out of plane and in plane) and the strain evolution in the CFRP strips during the explosion by means of two Photron SA5 high-speed cameras. The high-speed cameras are equipped with 50 mm focal length lenses and record at a frame rate of 30.000 fps with a resolution of 640X376 pixels. Two spotlights are positioned behind the cameras to improve the illumination of the set-up. A speckle pattern is applied on the specimens. The observed area is about 200x100 mm<sup>2</sup>. A subset size of 15x15 pixels is used with a subset spacing of 3 pixels. The 3D Vic software (version 2007) is used to determinate the motion of the subsets during the deformation. Two strain gauges of 20 mm length with a nominal resistance of 120  $\Omega$  are bonded at the fixed end of the CFRP strips. A strain gauge quarter bridge configuration is used, with respect to the built-in Wheatstone bridge in the data acquisition system. A linear variable transducer differential (LVDT) is fixed at the steel frame to monitor the vibration of the frame during the blast tests. Moreover, to monitor the out of plane vibration in the CFRP strip and the concrete prism, two shock accelerometers are glued to the sides of the concrete prism as shown in Figure 5. The red one is bonded at the free end of the CFRP strip and the blue one is glued at the end of the concrete prism in order to compare the frequency of vibration caused by the impact of the blast wave in the concrete prism and the CFRP strip.



#### High speed cameras for DIC measurement

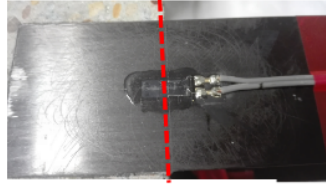
Photron SA5

Focal length lenses: 50 mm

Frame rate: 30 000 fps

Resolution: 640x376

The shutter speed: 54 000 1/s



#### Strain gauge

Gauge length: 20 mm

Gauge resistance: 120  $\Omega$



#### Shock accelerometers

Sensitivity: 0,01 m/s<sup>2</sup>

Measurement range:  $\pm 490\,000$  m/s<sup>2</sup>



#### LVDT

Sensitivity: 0,1 mm

Measurement range:  $\pm 150$  mm

Figure 5. Deformation measurement equipment

## 2.4 Blast load application

Some preliminary tests are performed to measure the reflected pressure signal at the end of the tube. Two pressure transducers type PCB102B are placed at the end of the tube and only one transducer is fixed on a rigid plate because of the small section of the tube. The physical admissible frequency of these pressure transducers are 500 kHz with an acquisition rate equals to 1MHz. An explosive charge of 20 g of C4 is fixed at the entrance of the tube with a zero-standoff distance. An average maximum reflected overpressure of 32.8 MPa and a specific impulse of 6365 Pa.s are obtained. The EDST and the resulting pressure temporal are shown in Figure 6.

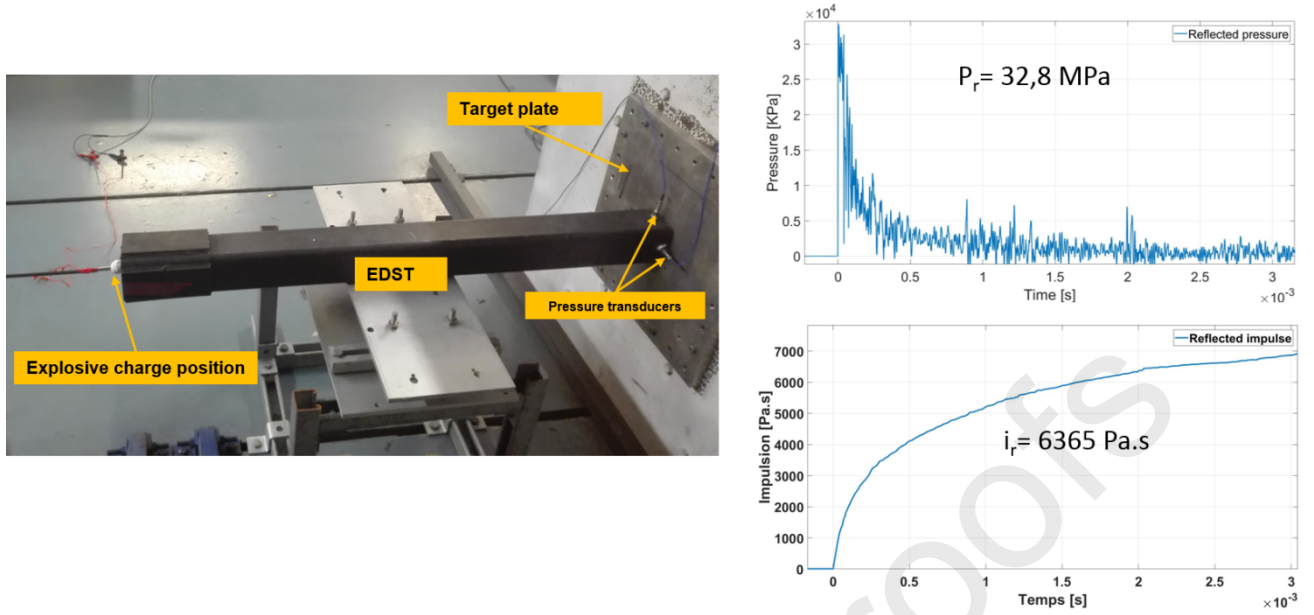


Figure 6. Image of the setup to measure the reflected pressure at the end of the tube

## 2.5 Experimental results

### 2.5.1 Maximum FRP force and failure aspect

The main test results, in terms of maximum FRP strain  $\varepsilon_{f, \max}$  (average values of 3 test repetitions) recorded at the loaded end by means of the strain gauges, the corresponding FRP force  $N_{f, \max}$  according to Equation 1 and the failure aspect are given in Table 2. Through the reaction force at the FRP anchorage has not been measured directly as part of the blast bond shear test, the maximum CFRP force ( $N_{f, \max}$ ) can be derived from the strain measurements at the loaded end of the CFRP as follows:

$$N_{f, \max} = \varepsilon_{f, \max} E_f A_f \quad (\text{Equation 1})$$

Where  $E_f$  is the young modulus of the CFRP strip and  $A_f$  is the cross section of the CFRP strip.

As indicated in table 2, the obtained strain is about 6 % to 14 % of the ultimate static tensile capacity of the CFRP strip. Yet, in reference to fib [19], the calculated force can also be compared to the predicted value of the maximum anchorage capacity under quasi-static loading ( $N_{fa \text{ stat}}$ ). The latter value can be calculated as follows:

$$\left\{ \begin{array}{l} \text{For bond length } l_b \geq l_{bmax}, N_{fa, stat1} = \alpha c_1 k_c k_b \sqrt{E_f t_f f_{ctm}} \quad (\text{Equation 2}) \\ \text{For bond length } l_b < l_{bmax}, N_{fa, stat2} = N_{fa, stat1} \frac{l_b}{l_{b,max}} \left(2 - \frac{l_b}{l_{b,max}}\right) \quad (\text{Equation 3}) \end{array} \right.$$

where

$$l_{b,max} = \sqrt{\frac{E_f t_f}{c_2 f_{ctm}}} \quad (\text{Equation 4})$$

and  $\alpha$  is a reduction factor, approximately equal to 0.9, to account for the influence of inclined cracks on the bond strength;  $k_c$  is a factor accounting for the state of compaction of concrete ( $k_c$  can generally be assumed to be equal to 1.0.  $c_1$  and  $c_2$  are equal to 0.64 and 2, respectively and  $k_b$  is a geometry factor:

$$k_b = 1.06 \sqrt{\frac{2 - \frac{b_f}{b}}{1 + \frac{b_f}{400}}} \quad (\text{Equation 5})$$

Note that  $b$ ,  $b_f$  and  $t_f$  are the width of the concrete prism, the width of the CFRP strip and the thickness of the CFRP strip, respectively and are measured in mm, and  $E_f$ ,  $f_{ctm}$  are the young modulus of the CFRP strip and the tensile strength of the concrete (see Table 1) and are measured in MPa.

Table 2. main test results

Specimens	Bond length [mm]	$\epsilon_{f, max}$ [ $\mu$ strain]	$N_{f, max}$ [kN]	$N_{fa, stat}$ [kN]	$\frac{N_{f, max}}{N_{fa, stat}}$	Failure aspect
A	50	1068	99.00	47.50	2.08	SC
B	100	1820	178.20	77.56	2.29	N/A
C	200	2340	231.66	90.68	2.55	N/A

\*N/A: not applicable (no failure); SC: shear cone bond failure

The same blast impulse is applied to all specimens and is resisted by the 2 CFRP strips of the double bond shear test configuration.

When increasing the bond length with the same blast impulse, increasing values of  $\epsilon_{f, max}$  are observed. An increase of 70 % and 119 % in the tensile strain is recorded for the specimens retrofitted with a bond length of 100 mm and 200 mm, respectively compared to the specimen with a bond length 50 mm. This is due to a combination of two aspects. With increasing the bond surface, total bond failure requires more energy to be damaged and thus takes more time to be achieved (e.g comparing specimens A and B in Table 2); yet the larger bond interface zone also increases the stiffness of the system, attracting a

large part of the blast energy to be taken by the CFRP (e.g comparing B and C in Table 2). Obtained values of  $\epsilon_{f, \max}$  in the blast bond test can be compared with the quasi static ultimate tensile strain of the CFRP ( $\epsilon_{fu, \text{stat}} = 1,7 \%$ ). Values are reported in Table 2 and vary between 6 % to 14 % of the static tensile capacity of the FRP.

Note that for given blast load and test configuration bond failure has been obtained for the 50 mm bond length specimens “A”, while bond failure could be avoided for the 100 mm and 200 mm bond length specimens “B and C”. This leads to the suggestion that for future blast bond shear testing a combination of bond length and blast impulse might be considered for test parameters. A particular bond failure has been obtained for specimens “A” as shown in Figure 7 and schematised in Figure 8



Figure 7. Debonding in the concrete prism for specimens A1, A2 and A3

For this short bond length a shear cone bond failure is obtained running in the concrete from the CFRP free end to the U shaped plate used to shield lateral impact of the blast wave on the CFRP directly.

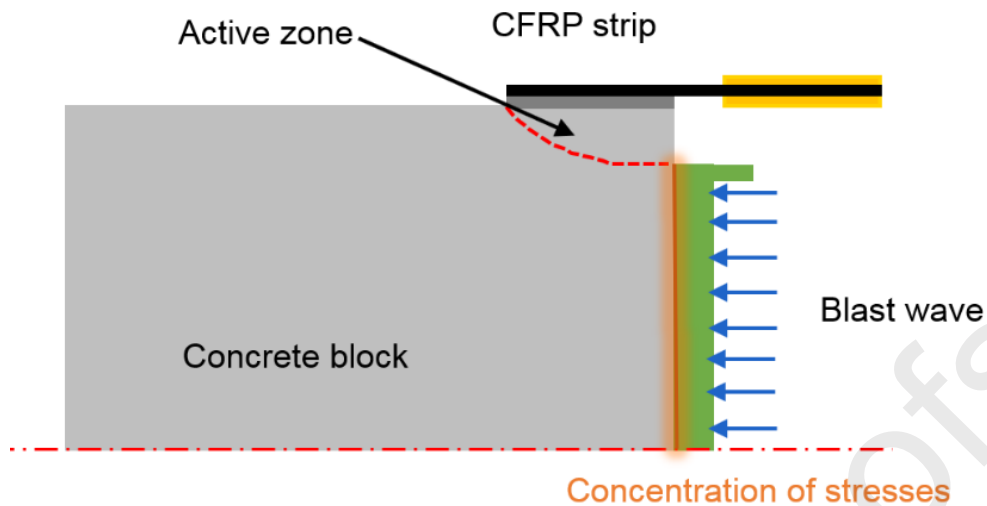


Figure 8. A schematic representation of the concrete shear failure

Increasing the bond length of the CFRP strips adds energy to the retrofitted concrete prisms to better resist to the blast loads due to the large zone involved to take up the dynamic stresses caused by the displacement of the concrete prism and the propagation of the blast wave within the concrete at the same time. This enhance of stiffness at CFRP-concrete interface is highlighted by the increase of the tensile strain in the CFRP strips.

### 2.5.2 Debonding process under blast loading

Under blast loading, the specimen doesn't have enough time to initiate micro cracks at the interface between the concrete and the CFRP strip as is the case for the static loading. At high loading rate, the strength of the prism's concrete is enhanced due to the strain rate effect and cracking runs through aggregates in the concrete prism as observed for specimens A (Fig. 7).

A high-speed camera is used to record the debonding process during the explosion. The recorded images show that the total debonding of the CFRP strips of specimens A occurs in a brittle and sudden manner.

Figure 9 shows the debonding process of one of the specimens with a bond length of 50 mm as follows:

(a) After the detonation, the blast wave hits the aluminium U-plate. This causes the displacement of the concrete prism. The displacement of the concrete prism causes a concentration of dynamic stresses at the interface between the CFRP strip and the concrete surface. Also shear stresses in the concrete are initiated as a results of the loading configuration (see previous section);

- (b) When the dynamic stresses state exceed the tensile strength of the concrete. A crack initiates at the free end of the CFRP;
- (c) Further, the development of the crack in the concrete propagates toward the U-shape plate resulting in failure via a concrete shear failure;
- (d) During the failure process, debris of concrete is observed.

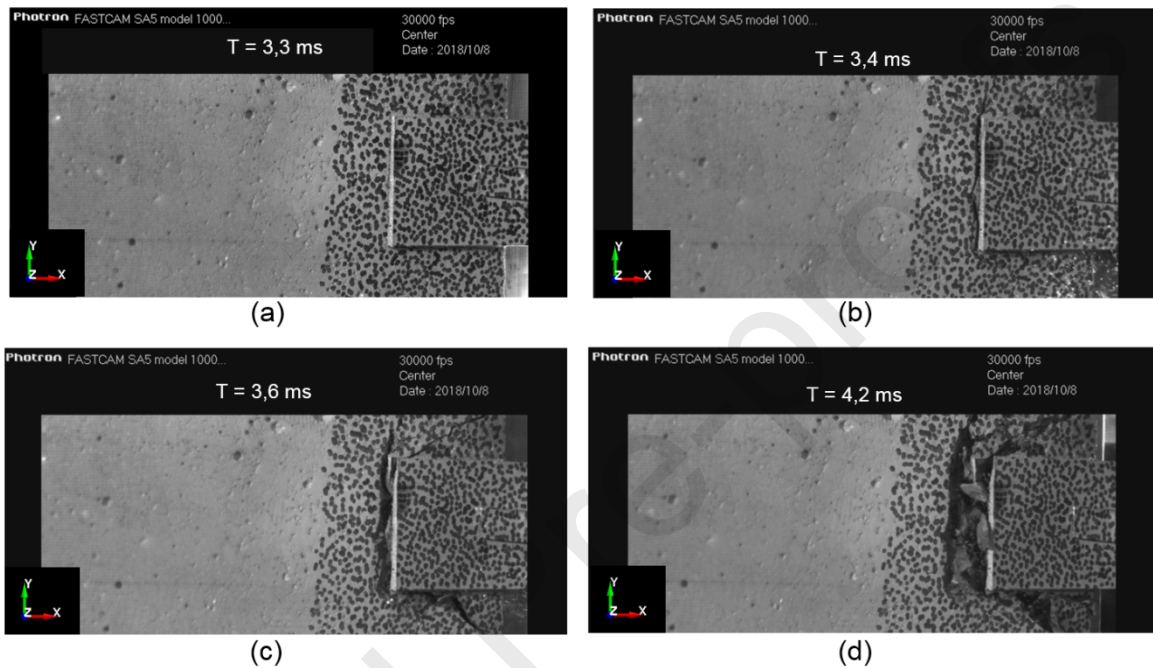


Figure 9. failure process in the concrete prism visualised by the high-speed camera.

The displacement of the CFRP strip and the concrete prism in different directions “X” (loading direction or horizontal displacement), “Y” (vertical displacement) and “Z” (out of plane displacement) are determined by DIC measurement. Two virtual points “F” and “G” are selected on the concrete prism and on the CFRP strip, respectively, as shown in Figure 10. A comparison of the displacement of these two points is provided in Figure 11.

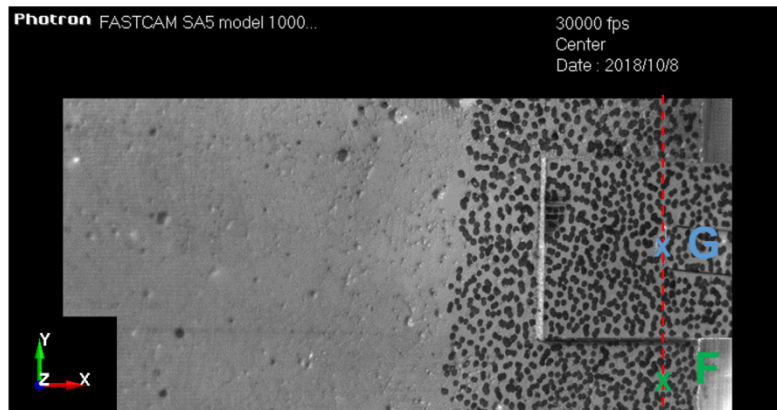


Figure 10. Position of the points “F” and “G” on the specimen’s surface

The debonding initiates at about 3.5 ms and is simultaneously observed in the three different directions, as shown in Figure 11. For the “X” direction, starting at time 3.3 ms the bonded CFRP strip and the concrete prism move together due to the impact of the blast wave. The debonding occurs when a maximum “X” displacement of 0.136 mm is reached. No displacement is recorded in the Y and Z directions until debonding occurs, which confirms that the aluminium U-plate prevents that the blast wave directly hits the lateral sides of the CFRP strips.

Consistent with the fact that no debonding is observed for the specimens with a bond length of 100 mm and 200 mm, both CFRP and concrete displacement remains the same for different directions. A maximum displacement of 0.147 mm is observed for the specimen B with a bond length of 100 mm. For specimen C, with bond length of 200 mm, a maximum “X” displacement of 0.063 mm is recorded. With increasing the bond length and keeping the same blast impulse a reduction of 58 % in the “X” displacement is recorded for the specimens C retrofitted with a bond length of 200 mm compared to the specimen B with a bond length 100 mm.

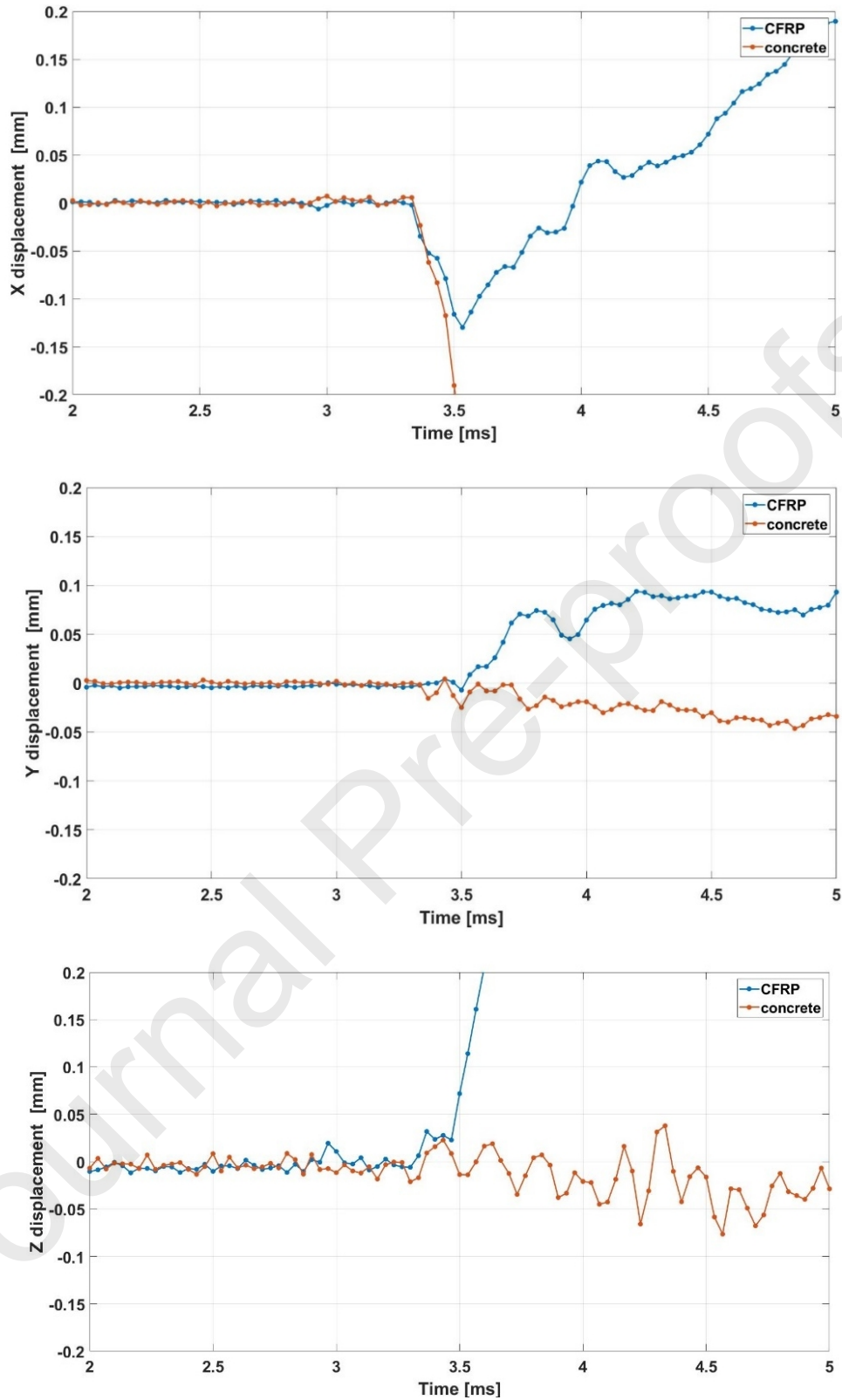


Figure 11. DIC measurements of the CFRP strip and concrete prism displacements in X,Y and Z directions for the specimen

“A”

Under blast loading, the bond interface between the CFRP strip and the concrete is activated due to a combined effect: (1) on the one hand the concentration of the shear and normal stresses caused by the propagation of the blast wave within the concrete bond interface and CFRP; (2) and on the other hand the stresses as a result of the displacement of the concrete prism relative to the CFRP. When this combination of dynamic stresses (normal and shear stresses) exceed the ultimate bond strength and the ultimate slip at the interface between the CFRP strip and concrete the debonding occurs.

The blast shear test set-up being designed to be compatible with the use of DIC measurements, allows to measure valuable data on the displacement field. Yet, this does not allow to characterize the relative contribution of both effects (propagation of the blast wave in the specimen versus relative displacement) and measures the combined effect. In this respect the combined use of experimental blast shear testing and finite element modelling might be considered.

### 2.5.3 Strain evolution along the bond length using DIC measurements

Using DIC measurements, the evolution of the strain along the bonded length are recorded during the explosion using virtual strain gauges. For 50 mm bond length, three virtual strain gauges are selected at different position as shown in Figure 12 . Where T1, T2 and T3 are the time steps when the concrete bloc starts to move, when the concrete bloc reaches a mid-displacement and when the concrete bloc reaches a maximum displacement, respectively. At T3, the CFRP strain shows a linear decay starting from the fixed end of the CFRP ( $x = 0$  mm) to the free end ( $x = 50$  mm). A maximum strain of 1013  $\mu$ strain is recorded at the delamination stage. At lower levels of displacements (T1 and T2) only a part of the bond length is activated.

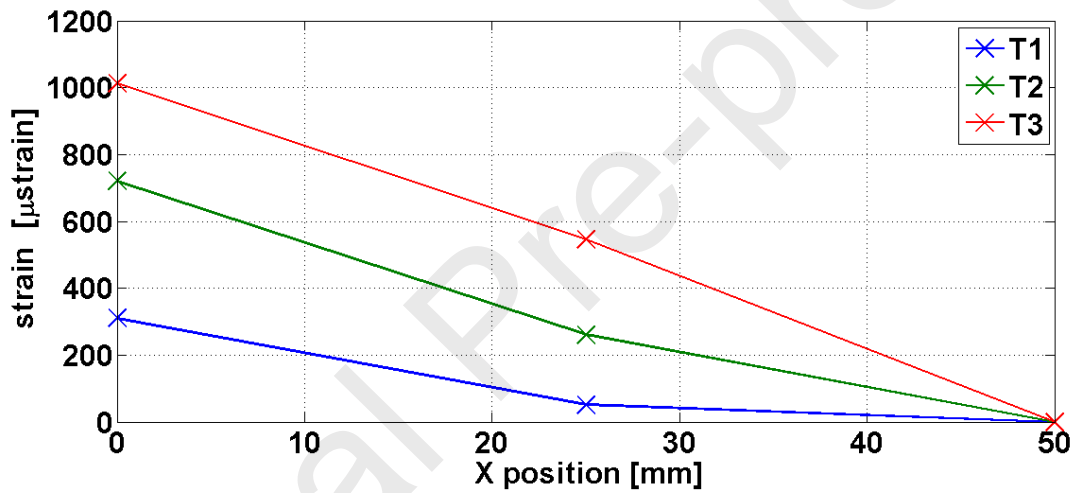
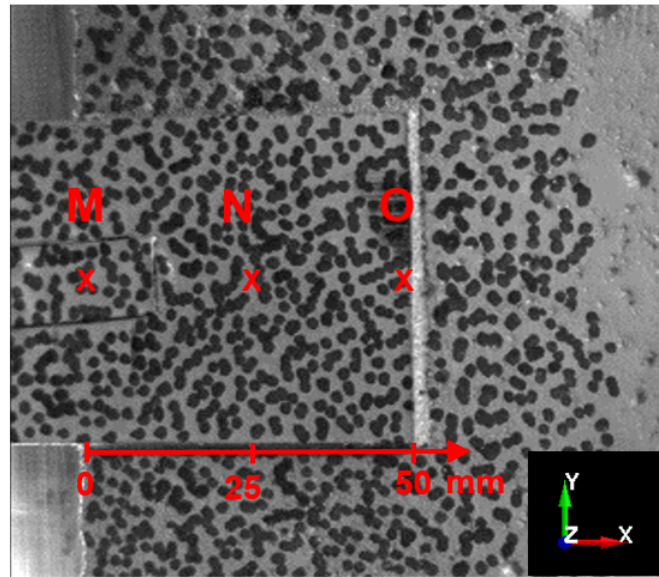


Figure 12. Strain evolution along the bond length of 50 mm using DIC measurements

For 100 mm bond length, the strain evolution in the CFRP strips is mainly concentrated near the loaded end of the CFRP strip and decreases along the bond length to the free end of the CFRP as shown in Figure 13. A maximum strain of 1720  $\mu\text{strain}$  near the fixed end is recorded using DIC measurements.

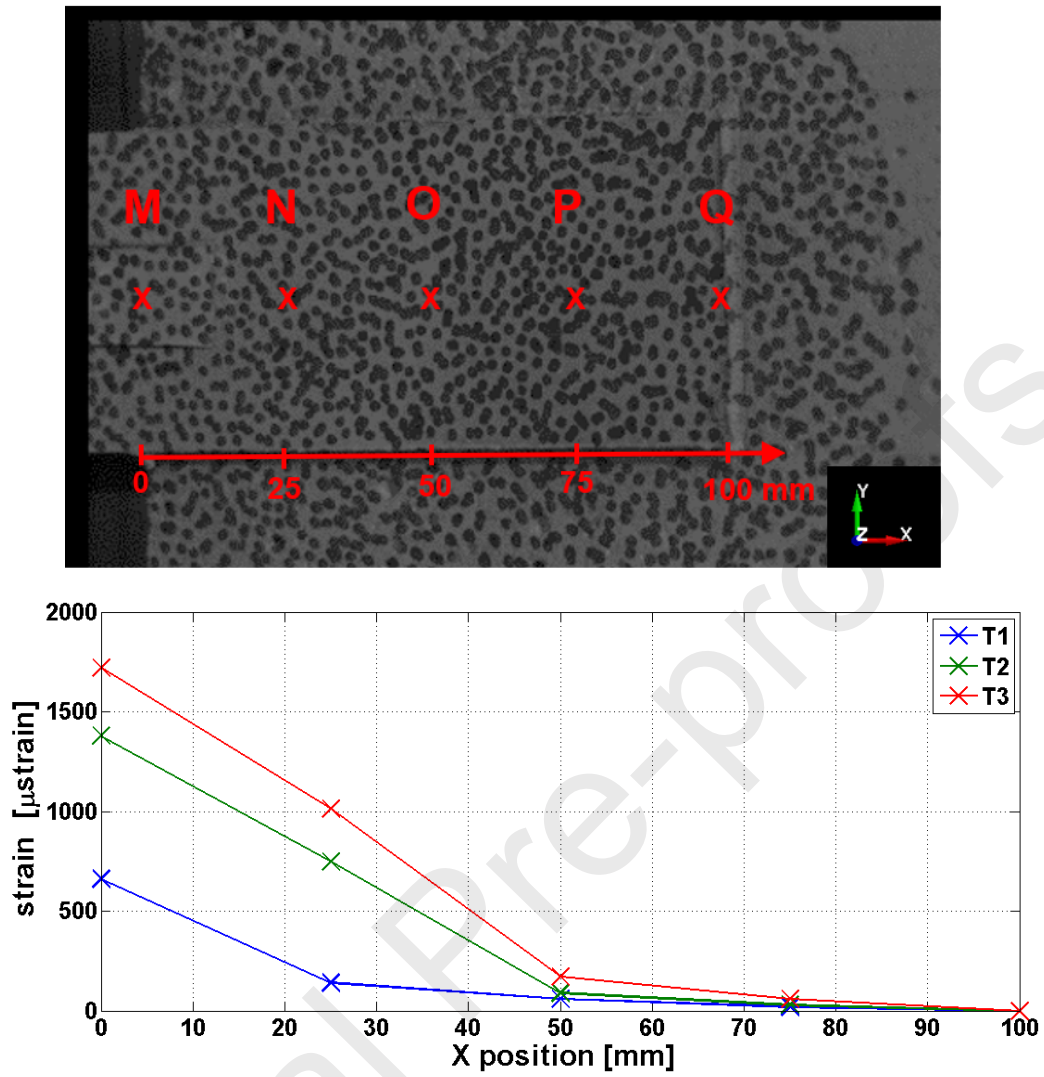


Figure 13. Strain evolution along the bond length of 100 mm using DIC measurements

Figure 14 shows the strain evolution in the CFRP strip along a bond length of 200 m. A maximum strain of 2482  $\mu$ strain near the fixed end is recorded using DIC measurements.

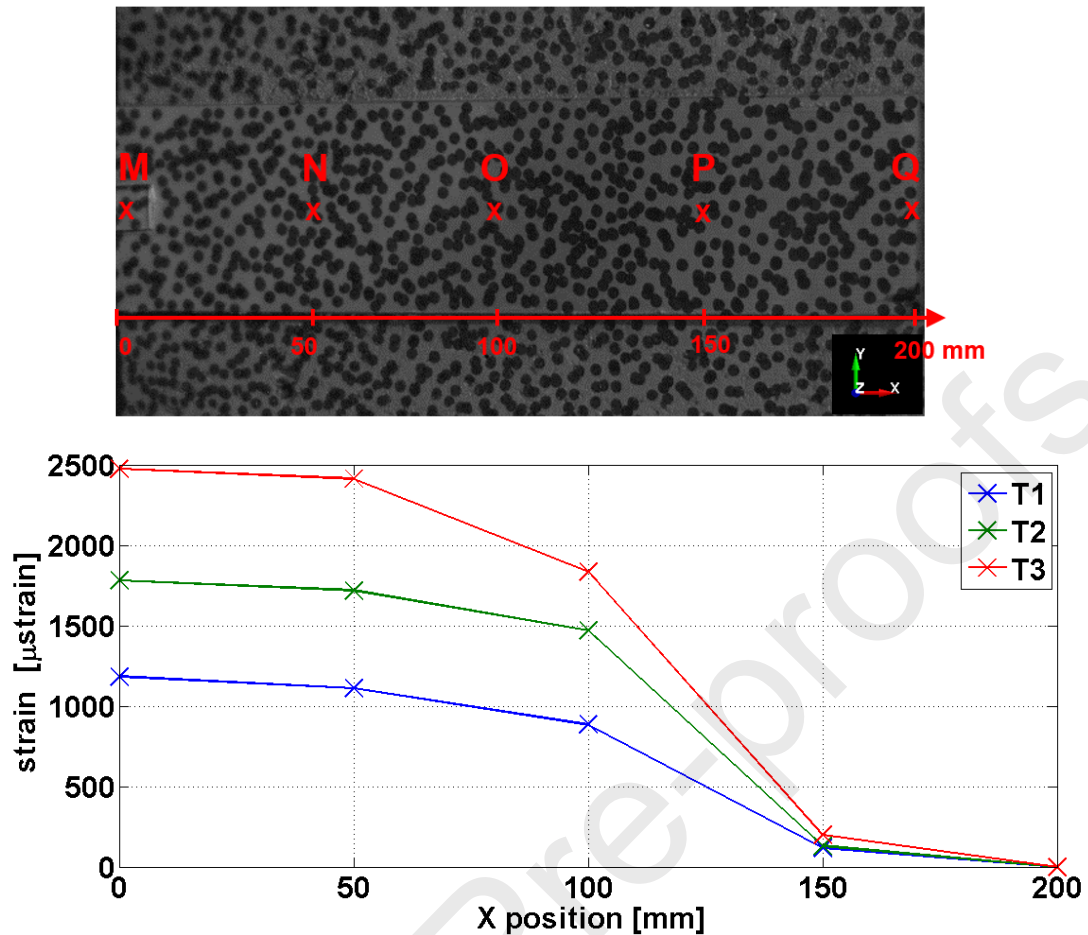


Figure 14. Strain evolution along the bond length of 200 mm using DIC measurements

#### 2.5.4 Strain evolution over time using electrical strain gauges

The variation of the strain in the CFRP strip at the loaded end is measured during the explosion using an electrical strain gauge for all the specimens. The results for specimen A1 with a bond length of 50 mm is shown in Figure 15. A peak tensile strain of 1067  $\mu$ strain is recorded due to the displacement of the concrete prism in “X” direction. In addition, vibrations are added due the propagation of the dynamic stresses in the CFRP strips. This explains the small oscillations recorded in the strain evolution over time. The strain in the CFRP strip drops down to zero around 0.5 ms and turns into a compressive strain at around 1.5 ms, this relates to the concrete shear failure as illustrated in Figure 7. Unfortunately, the strain gauges bonded on the specimens A2 and A3 are damaged during the debonding process.

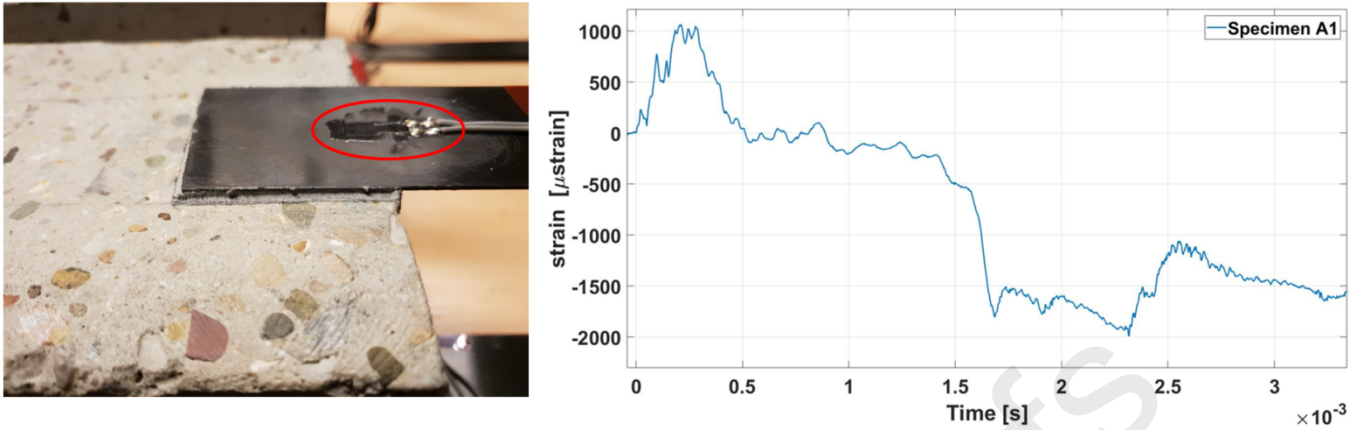


Figure 15. Evolution of the strain in the CFRP strip at the fixed end

For the specimens B1, B2 and B3 with a bond length of 100 mm, no debonding is observed in the experimental tests. The variation of the strain in the CFRP strip at the fixed end is measured during the explosion as shown in Figure 16. An average maximum tensile strain of 1820  $\mu$ strain is recorded during the inbound phase and a compressive strain of -505  $\mu$ strain is recorded during the rebound phase. The recorded maximum tensile strain corresponds to 10.7 % of the ultimate strain of the CFRP strip.

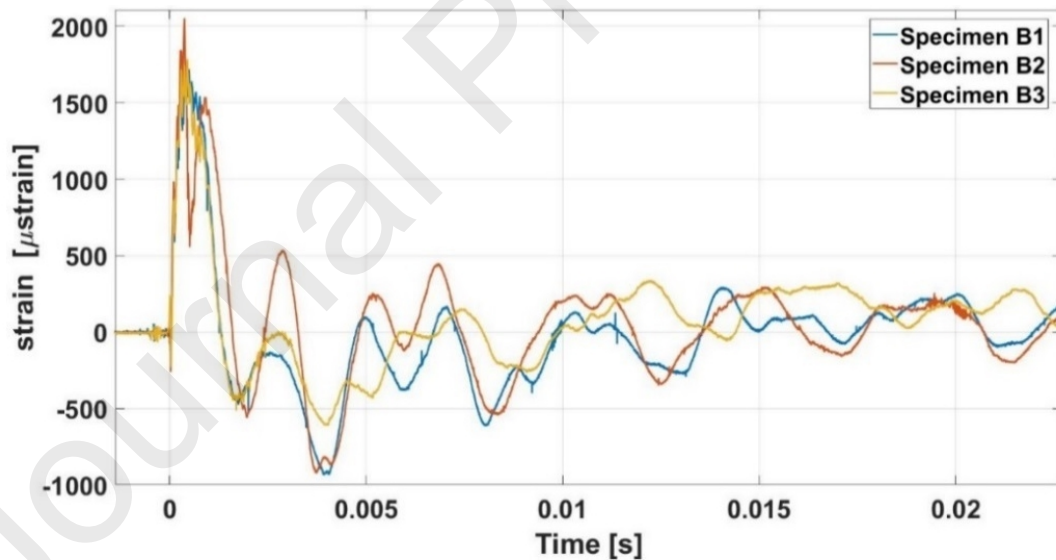


Figure 16. Strain evolution in the CFRP strips overtime for the specimens B

Also, for the specimens C1, C2 and C3 with a bond length of 200 m, no debonding is observed. The variation of the strain in the CFRP strip at the fixed end is measured during the explosion as shown in Figure 17. An average maximum tensile strain of 2340  $\mu$ strain is recorded during the inbound phase and

a compressive strain of  $-1080 \mu\text{strain}$  is recorded during the rebound phase. The recorded maximum tensile strain corresponds with 14.1 % of the ultimate strain of the CFRP strip.

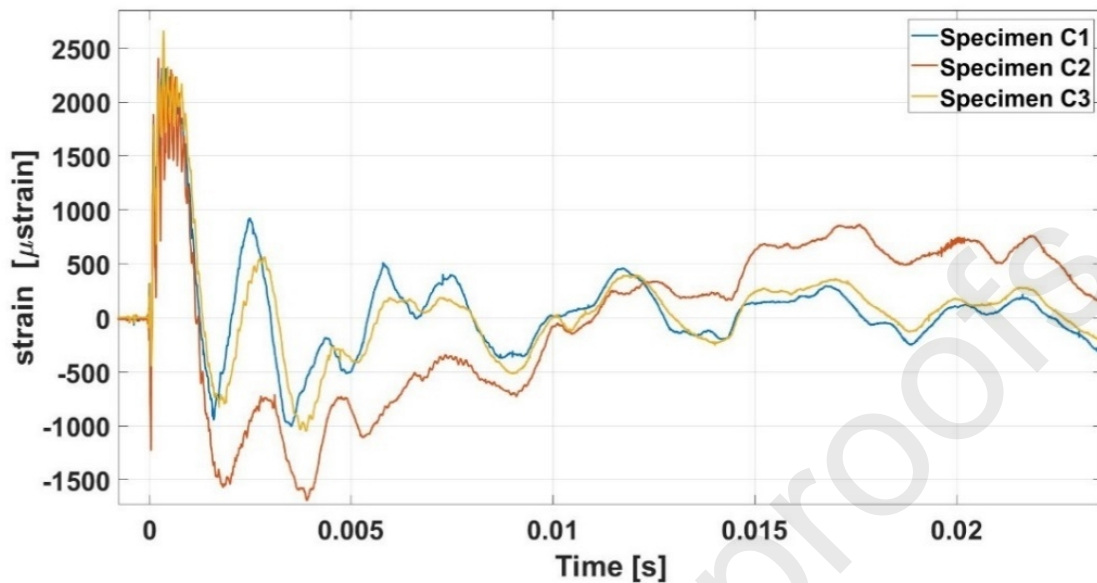


Figure 17. Strain evolution in the CFRP strips overtime for the specimens C

Due to the blast response, the concrete prisms are moving and vibrating, creating dynamic stresses at the interface between the concrete and the CFRP strips and resulting in failure for the specimens with a bond length of 50 mm. Mainly, the first peak (inbound) is of concern as this yields to the highest strains in the CFRP. Nevertheless, also the rebound stage can be of concern as the bond capacity for a compressive load situation might be less favourable (due to the direct normal stresses in tension to prevent to the bond interface from buckling). Conditional to the test configuration used in this study, the strains in the rebound stage appear sufficiently low not to trigger further debonding. Figure 18 shows a compression of the strain evolution over time between the specimens A1, B1 and C1.

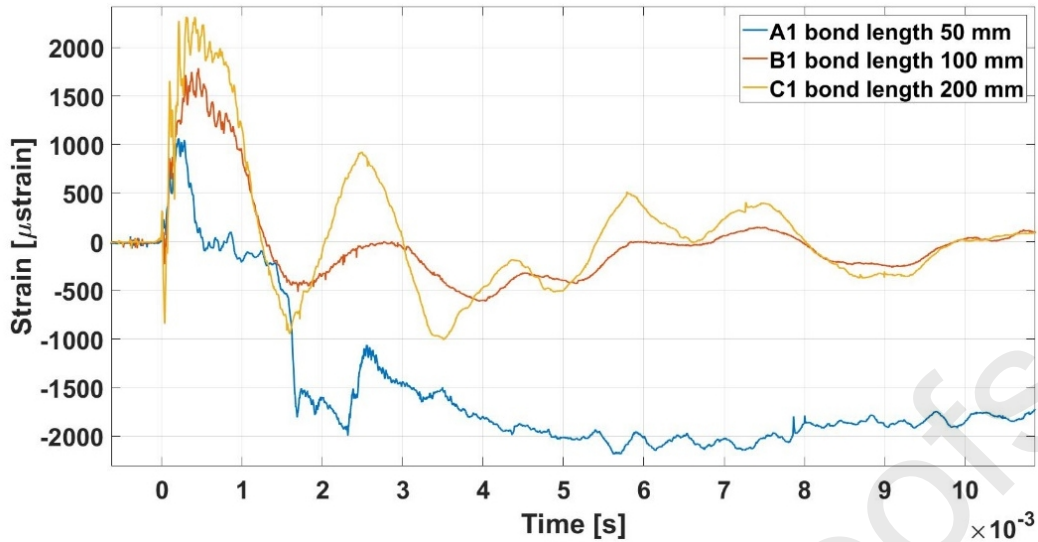


Figure 18. Evolution of the strain at the fixed end of the CFRP strip with different bond lengths

### 2.5.5 Out of plane vibration in the CFRP strip and concrete under blast loading

Figure 19 shows the evolution of the acceleration in “Z” direction. It can be noted that the propagation of the stress wave within the concrete and the CFRP strips generates out of plane vibration in the “Z” direction. The “Z” acceleration in the CFRP strips is totally different and higher than the “Z” acceleration in the concrete prisms in all retrofitted specimens with different bond length. This is surely explained by the different position of the shock accelerometer on the specimens. However, increasing the bond length reduces the vibration in the concrete prism and CFRP strip. A reduction of 41 % and 68 % of the Z acceleration in the concrete is recorded for the retrofitted specimens with a bond length of 100 mm and 200 mm, respectively compared with the specimen with a bond length of 50 mm. The propagation of the blast wave within the concrete and the CFRP strip generates normal stresses at the interface between the concrete and the CFRP strip causing out of plane vibrations.

Previous experimental shear tests between CFRP strips and concrete under quasi-static loading have shown that debonding usually occurs at the FRP-concrete interface with a thin layer of concrete remaining attached to the FRP [20–22]. Under static loading, bond slip tests between concrete and CFRP strip are mainly governed by the mode II (in plane shear). The stress-deformation relationship of the FRP-concrete interface is generally referred to as bond stress-slip law [23] since the deformation of interface is mainly the relative displacement (slip) between the FRP plate and the concrete prism.

Generally, this nonlinear relationship consists of two stages: an elastic stage in which the interfacial stress increases with the slip until it reaches a maximum value, and a softening stage in which interfacial stress decreases with the slip. However, for the blast loading the mixed modes (mode I and mode II) should be included as the propagation of the blast wave within the concrete causes out of plane stresses at the interface between the concrete and the CFRP strip. We believe that when the energy released by the explosion exceeds the fracture energy at the interface, debonding occurs.

Journal Pre-proofs

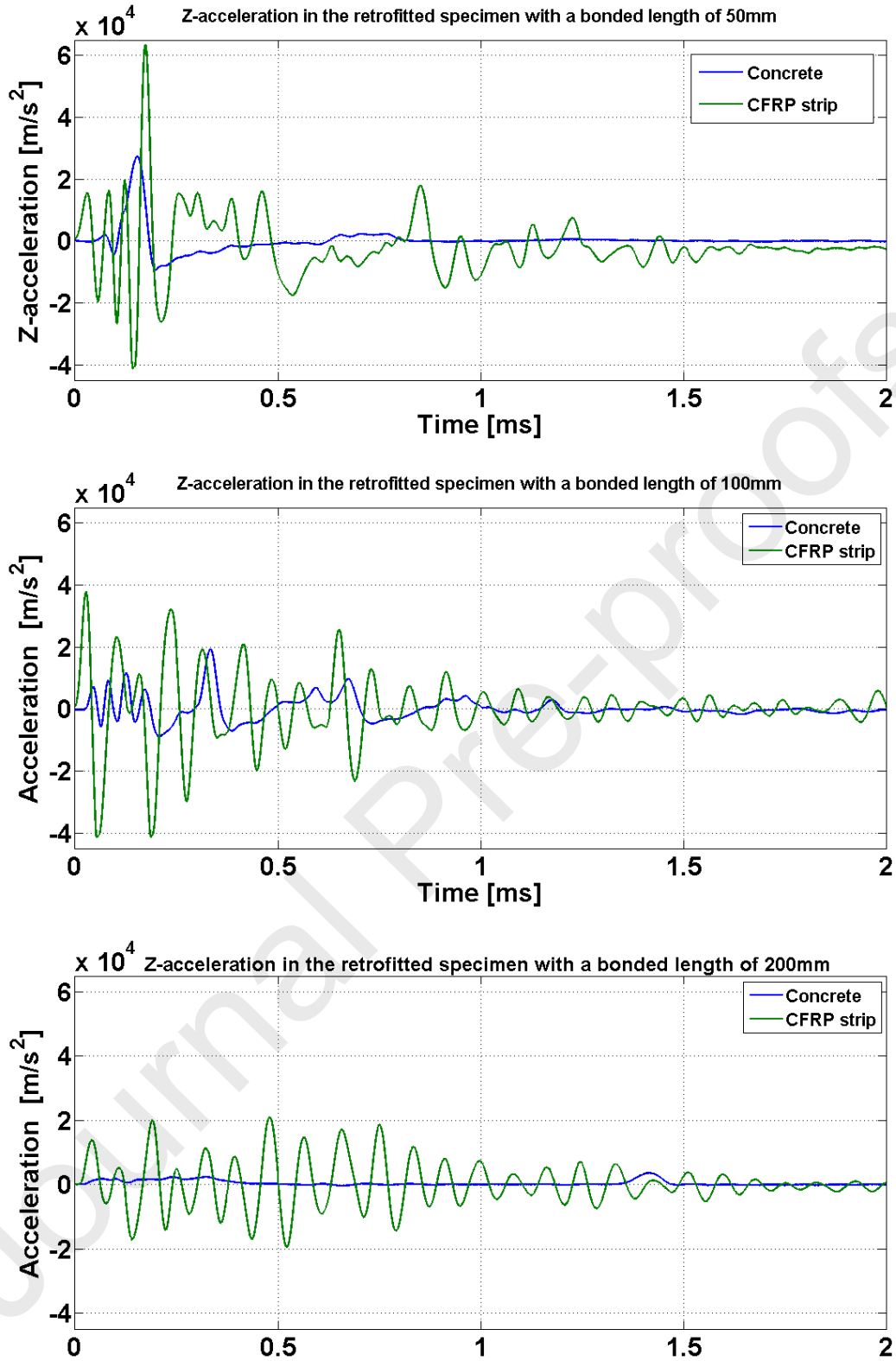


Figure 19. Evolution of the acceleration in the Z direction for the retrofitted specimens with different bond length

### 3. Conclusions

This study presents experimental results of the interfacial adhesive bond between CFRP strip and concrete under blast loading. In this respect double novel blast bond shear test set-up has been developed and first experience with the test configuration has been obtained through nine blast bond tests. The effect of propagation of the blast wave within the concrete is highlighted.

The conclusions from this study are as follows:

- Experimental tests demonstrate that under the considered blast loading applying the same reflected pressure and impulse, for the specimens “A” with a bond length of 50 mm, a concrete cone shear failure occurred while no bond failure was observed for longer bond length (100 mm, 200mm)
- The test configuration aimed at generating a combined effect in the blast shear test: (1) concentration of the shear and normal stresses at the interface caused by the propagation of the blast wave within the specimens and (2) stresses due to the displacement of the concrete prism at the same time.
- Increasing the bond length of the CFRP strips adds stiffness to the specimens and increases the strain distribution in the CFRP strips by taking part of the blast energy. An increase of 70 % and 119 % in the tensile strain is recorded for the specimens with a bond length of 100 mm and 200 mm, respectively compared to the specimen with a bond length 50 mm.
- The concrete strength of the concrete prism is enhanced due to the strain rate effect and cracking runs through aggregates in the concrete prism. Through a dynamic strength increase of the constituent materials under blast is typically the case, the bond interface stress field becomes also more complex and severe in case of blast.
- Under blast loading, the propagation of the blast wave through the concrete prism generates vibrations in different directions and increasing the bond length of the CFRP strip reduces the frequency of the out of plane vibration.

#### 4. References

- [1] Maazoun A, Belkassem B, Reymen B, Matthys S, Vantomme J, Lecompte D. Blast response of RC slabs with externally bonded reinforcement: experimental and analytical verification. *Compos Struct* 2018;200:1–21. <https://doi.org/10.1016/j.compstruct.2018.05.102>.
- [2] Maazoun A, Matthys S, Belkassem B, Lecompte D, Vantomme J. Blast response of retrofitted reinforced concrete hollow core slabs under a close distance explosion. *Eng Struct* 2019;191:447–59. <https://doi.org/10.1016/j.engstruct.2019.04.068>.
- [3] Crawford JE. State of the art for enhancing the blast resistance of reinforced concrete columns with fiber-reinforced plastic 1. *Can J Civ Eng* 2013;1033:1023–33. <https://doi.org/doi.org/10.1139/cjce-2012-0510>.
- [4] Jahami A, Temsah Y, Khatib J. The efficiency of using CFRP as a strengthening technique for reinforced concrete beams subjected to blast loading. *Int J Adv Struct Eng* 2019;11:411–20. <https://doi.org/10.1007/s40091-019-00242-w>.
- [5] Minor JK, Coleman TG, Orton SL, Vincent PC. Experimental Testing of CFRP-Strengthened Reinforced Concrete Slab Elements Loaded by Close-In Blast. *J Struct Eng* 2014;140. [https://doi.org/10.1061/\(ASCE\)ST.1943-541X.0000821](https://doi.org/10.1061/(ASCE)ST.1943-541X.0000821).
- [6] Youssf O, Elgawady MA, Mills JE, Ma X. Finite element modelling and dilation of FRP-confined concrete columns. *Eng Struct* 2014;79:70–85. <https://doi.org/10.1016/j.engstruct.2014.07.045>.
- [7] Tanapornraweekit G, Haritos N, Mendis P. Behavior of FRP-RC Slabs under Multiple Independent Air Blasts. *J Perform Constr Facil* 2011;25:433–40. [https://doi.org/10.1061/\(ASCE\)CF.1943-5509.0000191](https://doi.org/10.1061/(ASCE)CF.1943-5509.0000191).
- [8] Mosalam KM, Mosallam AS. Nonlinear transient analysis of reinforced concrete slabs subjected to blast loading and retrofitted with CFRP composites. *Compos Part B-Engineering* 2001;32:623–36. [https://doi.org/10.1016/S1359-8368\(01\)00044-0](https://doi.org/10.1016/S1359-8368(01)00044-0).
- [9] Ha JH, Yi NH, Choi JK, Kim JHJ. Experimental study on hybrid CFRP-PU strengthening effect on RC panels under blast loading. *Compos Struct* 2011;93:2070–82.

- <https://doi.org/10.1016/j.compstruct.2011.02.014>.
- [10] Nam JW, Kim HJ, Kim SB, Yi NH, Kim JHJ. Numerical evaluation of the retrofit effectiveness for GFRP retrofitted concrete slab subjected to blast pressure. *Compos Struct* 2010;92:1212–22. <https://doi.org/10.1016/j.compstruct.2009.10.031>.
- [11] Ghani Razaqpur A, Tolba A, Contestabile E. Blast loading response of reinforced concrete panels reinforced with externally bonded GFRP laminates. *Compos Part B Eng* 2007;38:535–46. <https://doi.org/10.1016/j.compositesb.2006.06.016>.
- [12] Lorenzis L De, Tegola A La. Bond of FRP laminates to concrete under impulse loading: a simple model. *Proc. Int. Symp. Bond Behav. FRP Struct.*, 2005, p. 495–500.
- [13] Buchan PA, Chen JF. Blast resistance of FRP composites and polymer strengthened concrete and masonry structures – A state-of-the-art review. *Compos Part B Eng* 2007;38:509–22. <https://doi.org/10.1016/j.compositesb.2006.07.009>.
- [14] Berthe L, Arrigoni M, Boustie M, Cuq-Lelandais JP, Broussillou C, Fabre G, et al. State-of-the-art laser adhesion test (LASAT). *Nondestruct Test Eval* 2011;26:303–17. <https://doi.org/10.1080/10589759.2011.573550>.
- [15] James RD, Paisley DL, Gruss KA, Parthasarathi S, Tittmann BR, Horie Y, et al. Adhesion evaluation of TiN and (Ti,Al)N coatings on titanium 6Al-4V. *Mater Res Soc Symp - Proc* 1996;410:377–82. <https://doi.org/10.1557/proc-410-377>.
- [16] Gay E, Berthe L, Buzaud E, Boustie M, Arrigoni M. Shock adhesion test for composite bonded assembly using a high pulsed power generator. *J Appl Phys* 2013;114. <https://doi.org/10.1063/1.4811696>.
- [17] Serbescu A, Guadagnini M, Pilakoutas K. Standardised double-shear test for determining bond of FRP to concrete and corresponding model development. *Compos Part B Eng* 2013;55:277–97. <https://doi.org/10.1016/j.compositesb.2013.06.019>.
- [18] Louar MA, Belkassem B, Ousji H, Spranghers K, Kakogiannis D, Pyl L, et al. Explosive driven shock tube loading of aluminium plates: Experimental study. *Int J Impact Eng* 2015;86:111–23. <https://doi.org/10.1016/j.ijimpeng.2015.07.013>.

- [19] fib. Externally bonded FRP reinforcement for RC structures. Bulletin 14, International Federation for Structural Concrete 2001.
- [20] Yao J, Teng JG, Chen JF. Experimental study on FRP-to-concrete bonded joints. *Compos Part B Eng* 2005;36:99–113. <https://doi.org/10.1016/j.compositesb.2004.06.001>.
- [21] Mazzotti C, Savoia M, Ferracuti B. An experimental study on delamination of FRP plates bonded to concrete. *Constr Build Mater* 2008;22:1409–21. <https://doi.org/10.1016/j.conbuildmat.2007.04.009>.
- [22] Lu XZ, Teng JG, Ye LP, Jiang JJ. Bond – slip models for FRP sheets / plates bonded to concrete. *Eng Struct* 2005;27:920–37. <https://doi.org/10.1016/j.engstruct.2005.01.014>.
- [23] Wang J. Cohesive zone model of FRP-concrete interface debonding under mixed-mode loading. *Int J Solids Struct* 2007;44:6551–68. <https://doi.org/10.1016/j.ijsolstr.2007.02.042>.

### **Author statement (Credit roles)**

1. **A. Maazoun:** Conceptualization, Methodology, Resources, Investigation, Formal analysis, Writing – Original draft, Writing – Review & Editing, Visualisation.
2. **S. Matthys:** Conceptualization, Methodology, Investigation, Formal analysis, Writing – Review & Editing, Resources, Supervision.
3. **B. Belkassem** Conceptualization, Methodology, Resources, Investigation.
4. **D. Lecompte:** Conceptualization, Methodology, Investigation, Formal analysis, Writing – Review & Editing, Resources, Supervision.
5. **O. Atoui:** Methodology, Resources, Investigation.

## **Experimental study of the bond interaction between CFRP and concrete under**

### **blast loading**

#### **Highlights :**

- The test configuration aimed in generating a combined effect in the blast shear test: (1) concentration of the shear and normal stresses at the interface caused by the propagation of the blast wave within the specimens and (2) stresses due to the displacement of the concrete prism at the same time.
- Increasing the bond length of the CFRP strips adds stiffness to the specimens and increases the strain distribution in the CFRP strips by taking part of the blast energy.
- The concrete strength of the concrete prism is enhanced due to the strain rate effect and cracking runs through aggregates in the concrete prism.
- Under blast loading, the propagation of the blast wave through the concrete prism generates vibrations in different directions and increasing the bond length of the CFRP strip reduces the frequency of the out of plane vibration.